



Background

Although endomysium with its relatively high turn-over is thought to be mechanically involved in force transmission, there is little knowledge about its regulatory determinants. Here, we report on the Master Athletic Laboratory Study of Intramuscular Connective Tissue (MALICoT, registration number DRKS00015764), which aims at determining the amount and composition of intramuscular connective tissue in human soleus muscle. To analyze the effects of physical activity and age, the healthy study participants were categorized into four groups comprising a group of young (20 to 35 years) non-physically active (n=12) subjects, a group of young power-trained athletes (n=10) as well as two groups of aged (60 to 75 years) subjects being either non-physically active (n=11) or power-trained athletes (n=10).

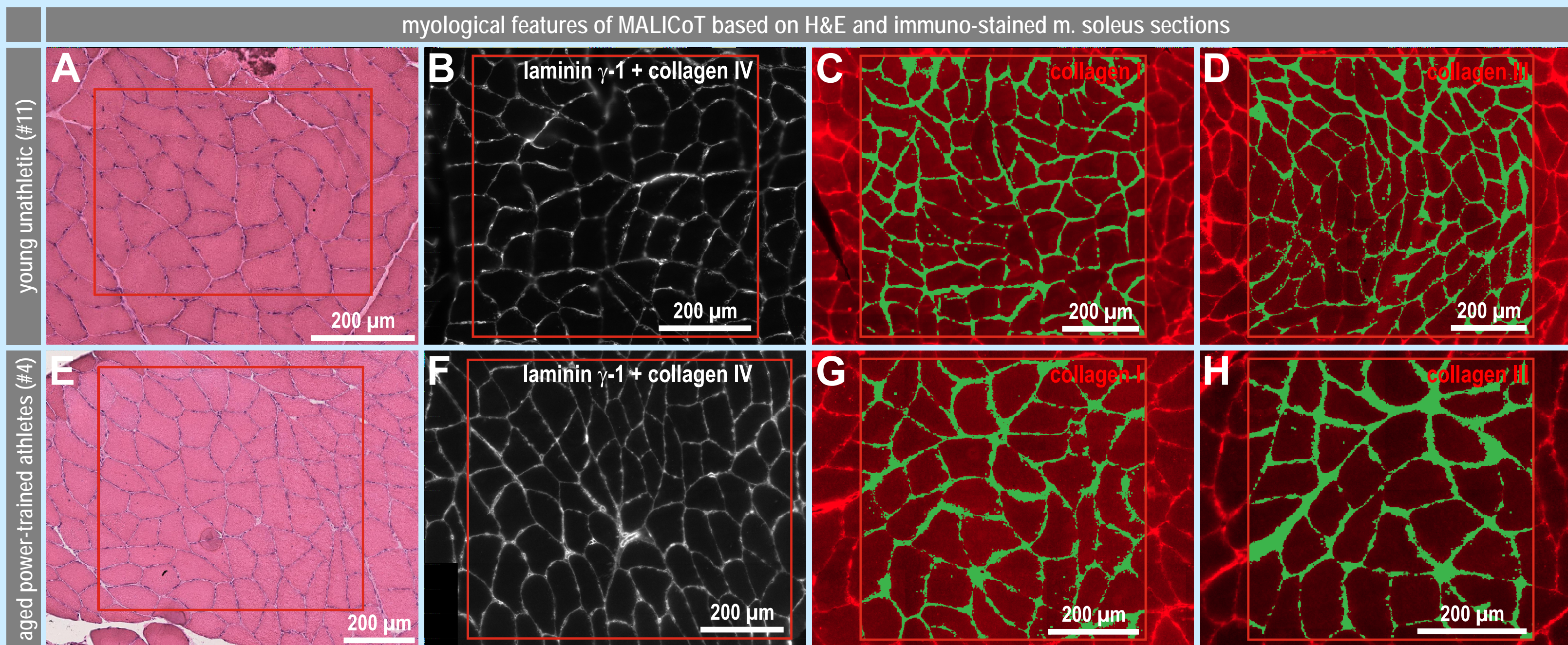
Methods

Biopsies from left soleus muscle from all participants were taken using a vacuum-assisted biopsy system (Vacora Biopsy System, Bard) with a 10G needle. The physical principle of this automated system with single-use biopsy needles is very similar to the manual Bergström biopsy technique [1,2]. We obtained 43 muscle biopsy specimens of approximately 19 mm length, 3 mm diameter, and 120 mg weight. Part of the tissue cylinders were mounted for transversal cryo-sectioning. Histologically stained soleus muscle sections underwent myopathological evaluation as well as an automated deep learning-based artificial intelligence biomedical image analysis [3]. Laminin- γ -1 and collagen IV double-stained as well as collagen I and III stained immunofluorescence images were digitally analyzed by standard microscopy software (Zeiss Zen v.3.4, Cell Profiler v.4.2.1) [4].

Results

Exemplary H&E and immunostained m. soleus sections of young & unathletic versus aged & power-trained athletes

myological features of MALICoT based on H&E and immuno-stained m. soleus sections

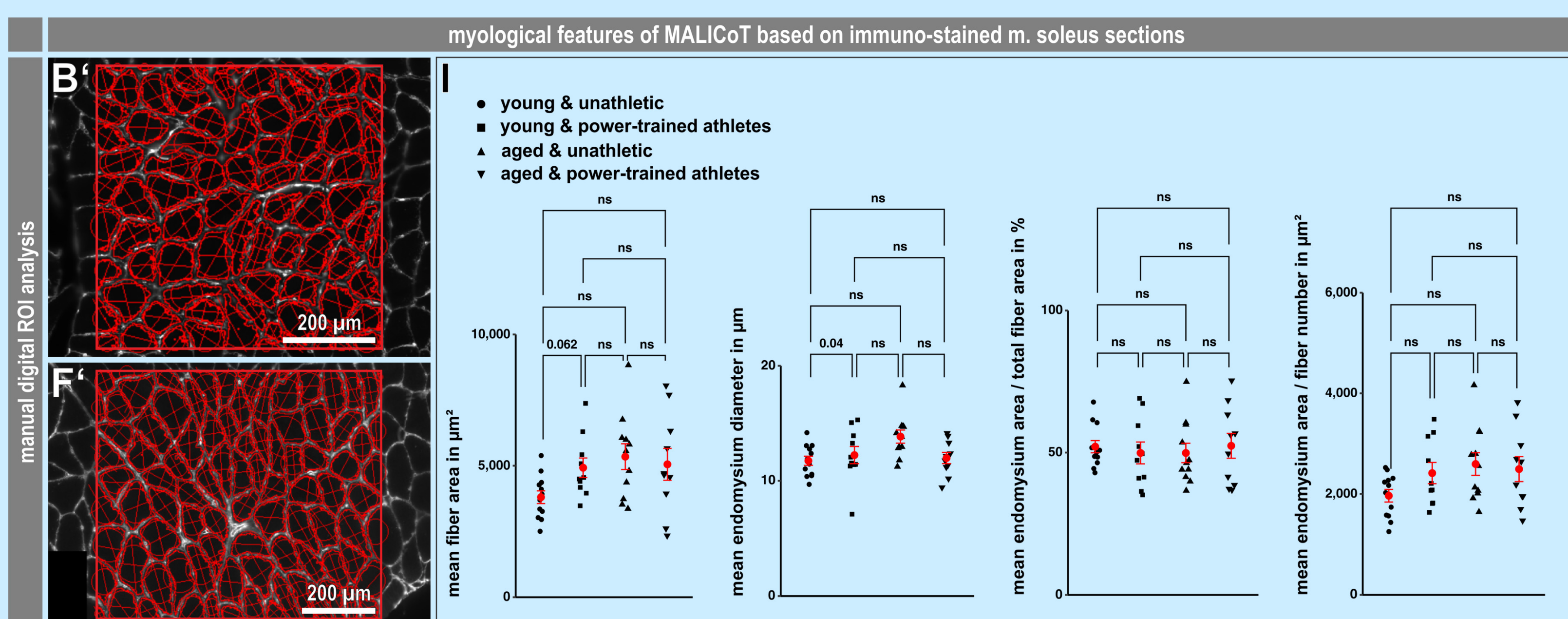


(A,E) H&E stained sections of human soleus muscle as used for evaluation by an experienced myopathologist (Table) as well as automated deep learning-based artificial intelligence biomedical image analysis for overall assessment and quantitation of muscle fiber area and endomysium content. For comparison, (B, F) laminin- γ -1/collagen IV double-immunostained as well as (C,G) collagen I and (D,H) collagen III immunostained sections of the same muscles were used for a manual digital image analysis.

Table: The spectrum of myopathological findings in the MALICoT study

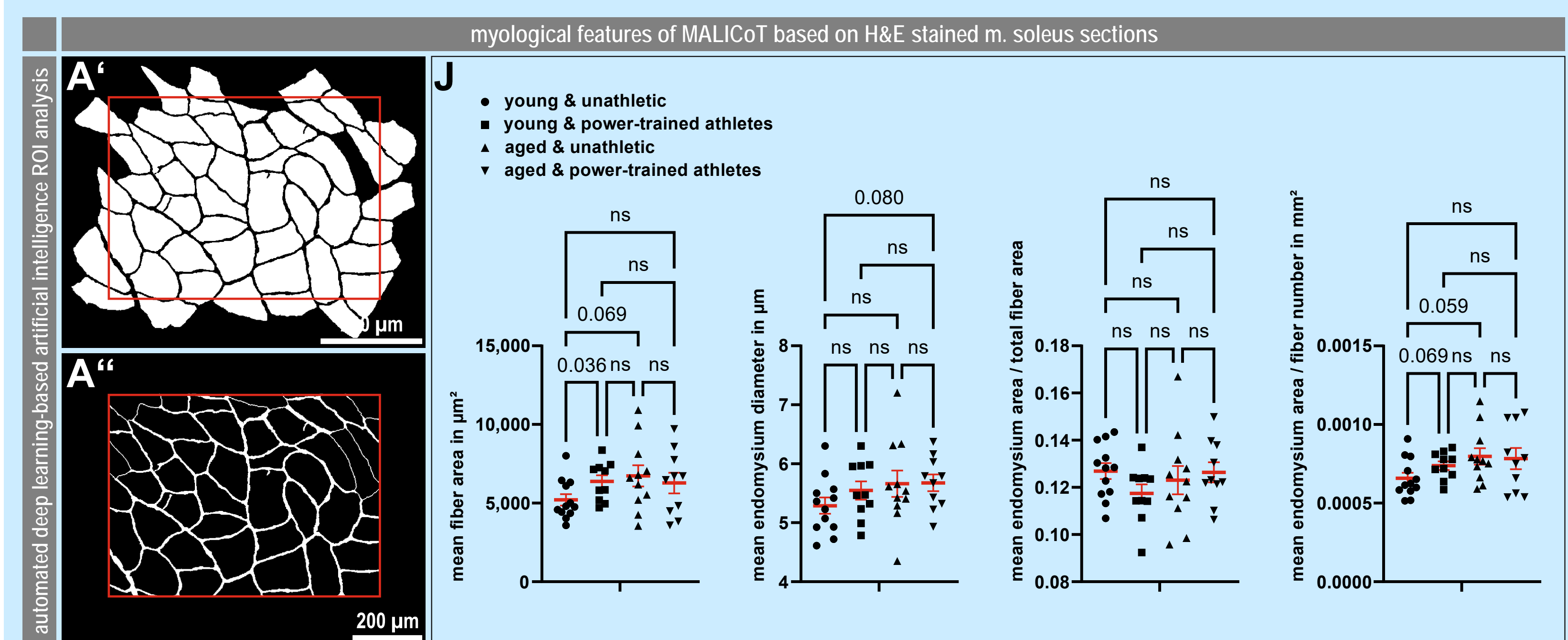
Subjects	Pathological findings	Key features from myological evaluation of H&E, Oil red O, GT, COX/SDH, PAS, MHCs, MHCf, MHCg, MHCn stained M. soleus sections						Diagnosis	
		Endomysial connective tissue	Oil red O pos. droplets	Ragged-red fibers	COX neg. fibers	Type I fibers	Type II fibers		MHCd/n pos. fibers
1	sporadic atrophic fibers	slight increase	middle-sized	0	0	~80-90%	~20%	1	
2	one atrophic fiber	slight increase	small-sized	0	0	~60%	~30-40%	1	
3	two nuclear clumps	slight increase	middle-sized	0	0	~80-90%	~30%	0	
4	sporadic atrophic fibers	normal	middle-sized	0	1	~80%	~30%	0	Unspec. myopathol. changes
5	none	slight increase	small-sized	0	0	~80-90%	~20-30%	2	
6	sporadic atrophic fibers, one nuclear clump	normal	small-sized	0	0	~70-80%	~20-30%	0	Unspec. myopathol. changes
7	sporadic atrophic fibers	slight increase	middle-sized	0	0	~70-80%	~20-40%	0	
8	sporadic atrophic fibers	slight increase	small-sized	0	1	~70-80%	~30-40%	3	
9	sporadic atrophic fibers	normal	small-sized	0	0	~90%	~10-20%	0	
10	sporadic atrophic fibers	slight increase	middle-sized	0	0	~60%	~40-50%	5	
11	sporadic atrophic fibers	normal	small-sized	0	0	~70-80%	~30-40%	0	
12	sporadic nuclear clumps	slight increase	small-sized	0	0	~80-90%	~20-30%	3	
1	none	normal	small-sized	0	0	~80%	~30%	0	
2	one degenerating fiber, one atrophic fiber	normal	middle-sized	0	0	~50%	~50%	2	
3	sporadic atrophic fibers, two nuclear clumps	slight increase	small-sized	0	0	~80%	~30%	0	Unspec. myopathol. changes
4	none	slight increase	small-sized	0	0	~70-80%	~30-40%	2	
5	sporadic atrophic fibers	slight increase	middle-sized	0	0	~70-80%	~20-30%	13	
6	sporadic atrophic fibers	slight increase	small-sized	0	0	~60%	~40-50%	0	
7	one degenerating fiber, multiple atrophic fibers, sporadic nuclear clumps	slight increase	middle-sized	0	1	~70%	~40-50%	35	
8	none	slight increase	middle-sized	0	1	~70-80%	~40-50%	0	
9	sporadic atrophic fibers	normal	small-sized	0	0	~80-90%	~30-40%	0	
10	sporadic atrophic fibers	slight increase	middle-sized	0	0	~70-80%	~20-30%	0	Unspec. myopathol. changes
1	sporadic atrophic fibers	slight increase	small-sized	0	0	~60%	~40%	8	Unspec. myopathol. changes
2	one degenerating fiber, multiple atrophic fibers, sporadic nuclear clumps, >3% fibers with centralised nuclei	slight increase	middle-sized	4	1	~70-80%	~30-40%	39	Chronic neurogenic atrophy
3	sporadic atrophic fibers, sporadic nuclear clumps	slight increase	small-sized	0	5	~80-90%	~20-30%	3	
4	sporadic atrophic fibers	normal	small-sized	0	0	~70-80%	~30%	4	
5	one nuclear clump	normal	small-sized	0	2	~70-80%	~20-30%	1	
6	sporadic atrophic fibers, >3% fibers with centralised nuclei	slight increase	small-sized	1	3	~60%	~40-50%	0	Unspec. myopathol. changes
7	sporadic atrophic fibers, sporadic nuclear clumps	slight increase	small-sized	0	0	~60%	~40-50%	3	
8	one regenerating fiber, groups of atrophic fibers, sporadic nuclear clumps	normal	middle-sized	0	1	~90%	~20-30%	12	
9	sporadic atrophic fibers	normal	small-sized	0	2	~70%	~30-40%	4	Unspec. myopathol. changes
10	sporadic nuclear clumps	normal	small-sized	0	1	~70-80%	~40-50%	11	
11	sporadic atrophic fibers, sporadic nuclear clumps	slight increase	small-sized	0	3	~90%	~30-40%	0	
1	one regenerating fiber, sporadic atrophic fibers	slight increase	coarse-sized	0	0	~100%	~10%	7	Beginning type II fiber atrophy
2	sporadic atrophic fibers	slight increase	small-sized	1	3	~80%	~40%	12	Unspec. myopathol. changes
3	sporadic atrophic fibers	slight increase	small-sized	1	0	~90-100%	~10-20%	14	Unspec. myopathol. changes
4	two atrophic fibers, two nuclear clumps	slight increase	small-sized	0	0	~90%	~15%	10	Unspec. myopathol. changes
5	sporadic atrophic fibers	normal	small-sized	0	0	~90%	~10%	0	Unspec. myopathol. changes
6	one endomysial and one perimysial inflammatory infiltrate, groups of atrophic fibers, sporadic nuclear clumps, >3% fibers with centralised nuclei	slight increase	coarse-sized	3	2	~90%	~10%	18	Unspec. myositic changes
7	sporadic atrophic fibers, one nuclear clump	slight increase	small-sized	0	0	~80%	~10%	16	Unspec. myopathol. changes
8	one regenerating fiber, groups of atrophic fibers, sporadic nuclear clumps	slight increase	middle-sized	0	1	~90%	~20-30%	18	Chronic neurogenic atrophy
9	sporadic regenerating fibers, sporadic atrophic fibers, sporadic nuclear clumps	slight increase	small-sized	1	0	~70-80%	~30-40%	10	Chronic neurogenic atrophy
10	one regenerating fiber, sporadic nuclear clumps	normal	small-sized	0	0	~80%	~30-40%	7	Chronic neurogenic atrophy

Quantitation of endomysial connective tissue by manual digital image analysis depicts increased endomysium in aged subjects irrespective of training status



(B',F') Exemplary laminin- γ -1/collagen IV double-immunostained sections of the above images (B,F) with fiber masks derived from manual digital image annotation. (I) Using this kind of quantitative image analysis approach, no statistical significance could be determined for the main features 'mean fiber area', 'mean endomysium diameter', 'mean endomysium area to total fiber area ratio', and 'mean endomysium area to fiber number ratio'. However, note the influence of age on 'mean fiber area' and the two endomysium to fiber ratios.

Quantitation of endomysial connective tissue by automated deep learning-based artificial intelligence image analysis depicts increased endomysium with physical activity and age



(A',A'') Exemplary fiber and endomysium masks of the above H&E image (A) derived from automated deep learning-based artificial intelligence image annotation. (J) Using this advanced quantitative image analysis approach, we noted statistically significant effects of physical activity as well as age on the main features 'mean fiber area', 'mean endomysium diameter', and 'mean endomysium area to fiber number ratio'.

Affiliations & References

- Institute of Aerospace Medicine, German Aerospace Center (DLR), Cologne, Germany
- MIRA Vision Microscopy GmbH, Eisingen/Fils, Germany
- Department of Neuropathology, University Hospital Erlangen, Friedrich-Alexander-University Erlangen-Nürnberg, Erlangen, Germany

- C.C. Lee, et al., J. Wanagat, Enhanced Methods for Needle Biopsy and Cryopreservation of Skeletal Muscle in Older Adults, J Cytol Histol 11 (2020)
- S.N. Akarolo-Anthony, et al., C.A. Adebamowo, Office based muscle biopsy using Vacora vacuum assisted biopsy system, Afr J Med Med Sci 41 (2012) 313-316
- L. Mill, et al., A. Grüneboom, SYNTA: A novel approach for deep learning-based image analysis in muscle histopathology using photo-realistic synthetic data, (2022) doi.org/10.48550/arXiv.2207.14650
- G.K. Thot, C. Berwanger, et al., J. Rittweger, Effects of long-term immobilisation on endomysium of the soleus muscle in humans, Exp Physiol 106 (2021) 2038-2045

Correspondence to carolin.berwanger@dlr.de, joern.rittweger@dlr.de, and christoph.clemen@dlr.de

Conclusion

In contrast to the time-consuming analysis of muscle fiber and connective tissue features by e.g. fluorescence imaging in conjunction with manual digital image analysis, the fast and automated deep learning-based artificial intelligence image analysis of standard H&E stained muscle sections depicted statistically significant changes features. Notably, physical activity led to increased 'mean fiber area' and increased 'mean endomysium area to fiber number ratio'. This new image analysis approach offers a fast, easy to handle, extendable, quantitative, and reliable solution to address connective tissue content and other features in human skeletal muscle biopsy samples.